

**Hiroharu Takenaka, Mitsuru Horiba, Hisaaki Ishiguro, Arihiro Sumida, Mayumi Hojo, Akihiko Usui, Toshiaki Akita, Sadatoshi Sakuma, Yuichi Ueda, Itsuo Kodama and Kenji Kadomatsu**

*Am J Physiol Heart Circ Physiol* 296:462-469, 2009. First published Dec 5, 2008;  
doi:10.1152/ajpheart.00733.2008

**You might find this additional information useful...**

---

This article cites 39 articles, 19 of which you can access free at:

<http://ajpheart.physiology.org/cgi/content/full/296/2/H462#BIBL>

This article has been cited by 2 other HighWire hosted articles:

**Midkine gene transfer after myocardial infarction in rats prevents remodelling and ameliorates cardiac dysfunction**

A. Sumida, M. Horiba, H. Ishiguro, H. Takenaka, N. Ueda, H. Ooboshi, T. Opthof, K. Kadomatsu and I. Kodama

*Cardiovasc Res*, January 19, 2010; 0 (2010): cvp386v2-cvp386.

[\[Abstract\]](#) [\[Full Text\]](#) [\[PDF\]](#)

**Kidney calling lung and call back: how organs talk to each other**

J. Floege and S. Uhlig

*Nephrol. Dial. Transplant.*, January 1, 2010; 25 (1): 32-34.

[\[Full Text\]](#) [\[PDF\]](#)

Updated information and services including high-resolution figures, can be found at:

<http://ajpheart.physiology.org/cgi/content/full/296/2/H462>

Additional material and information about *AJP - Heart and Circulatory Physiology* can be found at:

<http://www.the-aps.org/publications/ajpheart>

---

This information is current as of January 20, 2010 .

## Midkine prevents ventricular remodeling and improves long-term survival after myocardial infarction

Hiroharu Takenaka,<sup>1,4\*</sup> Mitsuru Horiba,<sup>4\*</sup> Hisaaki Ishiguro,<sup>2,4</sup> Arihiro Sumida,<sup>4</sup> Mayumi Hojo,<sup>4</sup> Akihiko Usui,<sup>1</sup> Toshiaki Akita,<sup>1</sup> Sadatoshi Sakuma,<sup>5</sup> Yuichi Ueda,<sup>1</sup> Itsuo Kodama,<sup>4</sup> and Kenji Kadomatsu<sup>3</sup>

Departments of <sup>1</sup>Cardiothoracic Surgery, <sup>2</sup>Cardiology, and <sup>3</sup>Biochemistry, Nagoya University Graduate School of Medicine; <sup>4</sup>Department of Cardiovascular Research, Research Institute of Environmental Medicine, Nagoya University, Nagoya; and <sup>5</sup>Cell Signals Incorporated, Yokohama, Japan

Submitted 15 July 2008; accepted in final form 18 November 2008

**Takenaka H, Horiba M, Ishiguro H, Sumida A, Hojo M, Usui A, Akita T, Sakuma S, Ueda Y, Kodama I, Kadomatsu K.** Midkine prevents ventricular remodeling and improves long-term survival after myocardial infarction. *Am J Physiol Heart Circ Physiol* 296: H462–H469, 2009. First published December 5, 2008; doi:10.1152/ajpheart.00733.2008.—Cardiac remodeling is thought to be the major cause of chronic heart dysfunction after myocardial infarction (MI). However, molecules involved in this process have not been thoroughly elucidated. In this study we investigated the long-term effects of the growth factor midkine (MK) in cardiac remodeling after MI. MI was produced by ligation of the left coronary artery. MK expression was progressively increased after MI in wild-type mice, and MK-deficient mice showed a higher mortality. Exogenous MK improved survival and ameliorated left ventricular dysfunction and fibrosis not only of MK-deficient mice but also of wild-type mice. Angiogenesis in the peri-infarct zone was also enhanced. These *in vivo* changes induced by exogenous MK were associated with the activation of phosphatidylinositol 3-kinase (PI3K)/Akt and MAPKs (ERK, p38) and the expression of syndecans in the left ventricular tissue. *In vitro* experiments using human umbilical vein endothelial cells confirmed the potent angiogenic action of MK via the PI3K/Akt pathway. These results suggest that MK prevents the cardiac remodeling after MI and improves the survival most likely through an enhancement of angiogenesis. MK application could be a new therapeutic strategy for the treatment of ischemic heart failure.

growth factor

ISCHEMIC HEART DISEASE (IHD) remains a leading cause of morbidity and mortality in many industrialized countries. Current treatment options for patients with advanced IHD include medical therapy or coronary revascularization by percutaneous coronary angioplasty or coronary bypass graft surgery (33). In a significant number of IHD patients, however, the standard revascularization therapies do not improve their clinical outcome. Induction of neovascularization by molecular biological procedures is expected to be a valid approach to ameliorate the pathophysiological changes in the ventricles of IHD. Transfer of angiogenic genes, cell implantation, and the administration of some growth factor proteins were reported to induce angiogenesis, leading to a prevention of cardiac fibrosis and resultant contractile dysfunction in animal IHD models (39). Most double-blind placebo-controlled clinical trials to date, however, failed to demonstrate sufficient efficacy of these procedures (11, 34).

\* H. Takenaka and M. Horiba contributed equally to this work.

Address for reprint requests and other correspondence: K. Kadomatsu, Dept. of Biochemistry, Nagoya Univ. Graduate School of Medicine, Tsurumai-cho, Showa-ku, Nagoya 466-8550, Japan (e-mail: kkadoma@med.nagoya-u.ac.jp).

Midkine (MK) is a heparin-binding growth factor with a molecular weight of 13 kDa, first isolated as the product of a retinoic acid-responsive gene in an embryonal carcinoma cell differentiation system, and is rich in basic amino acids and cysteine (15, 16). Structurally, MK shares ~50% sequence homology with pleiotrophin/heparin-binding growth-associated molecule (PTN/HB-GAM) but is not related to other growth factors or neurotrophic factors. The mouse MK and human MK have more than 90% homology (23), and human MK showed significant effects for mouse *in vivo* models (12, 13). MK has various biological activities; it promotes neurite outgrowth, survival of embryonic neurons, fibrinolytic activity of endothelial cells, and the migration of inflammatory leukocytes. MK is expressed strongly in early as well as advanced stages of tumors and involved in carcinogenesis and tumor progression. MK could have an angiogenic action on the ischemic heart because MK was shown to increase vascular density in tumorigenesis (4). The present study was designed to test this hypothesis in mouse models of myocardial infarction (MI). We have found that endogenous MK is responsible for adaptive angiogenesis in the heart after MI by regulating the activation of phosphatidylinositol 3-kinase (PI3K)/Akt and MAPKs. Exogenous application of MK was shown to improve cardiac function and survival of the post-MI mice through prevention of left ventricle (LV) remodeling. Notably, this improvement was observed not only in MK-deficient (MKKO) mice but also in wild-type (WT) mice.

### MATERIALS AND METHODS

**Mouse models.** All animal experiments were performed in accordance with the regulations adopted by National Institutes of Health and approved by the Animal Care and Use Committee of Nagoya University. MKKO mice were generated as described elsewhere (25). Adult male C57BL/6 (WT) and male MKKO mice with the C57BL/6 genetic background were used in either ischemic-reperfusion or a ligation model of MI (age, 10–12 wk old; and weight, 22–25 g) and were fed normal rodent chow. Mice were anesthetized with pentobarbital (100 mg/kg ip) and ventilated through a nose cone with a tidal volume of 0.2 ml at 120 breaths/min using a rodent respirator (model SN-480-7; Shinano, Tokyo, Japan). The extremity leads of the ECGs were monitored continuously. A thoracotomy was performed in the left third intercostal space, and the beating heart was exposed. An 8-0 polypropylene suture was passed under the left coronary artery at the inferior edge of the left atrium and tied with a slipknot to

The costs of publication of this article were defrayed in part by the payment of page charges. The article must therefore be hereby marked “advertisement” in accordance with 18 U.S.C. Section 1734 solely to indicate this fact.

produce occlusion. Myocardial ischemia was verified by blanching of the LV and ST elevation in ECGs. Air was then evacuated from the chest cavity, and the chest was closed with the ends of the slip outside of the incision. The ventilator was then removed, and normal respiration was restored. The blood samples of mice at 24 h after ischemic-reperfusion or the ligation procedure were collected from tail veins (0.2 ml each), and serum cardiac troponin T (cTnT) levels were measured to estimate the initial MI size (SRL, Tokyo, Japan). The animals were euthanized 7–28 days after the surgical operation.

For the *in vivo* MK treatment experiments, MK protein in saline (1 mg/ml) was subcutaneously infused for 7–28 days by using an osmotic pump (Alza, Palo Alto, CA). As the control, saline was infused by the pump. The pumps were implanted under the abdominal skin and exchanged in each 7 days.

**Histology.** Mouse hearts were embedded in paraffin after fixation with 4% paraformaldehyde and were cut into 5- $\mu$ m sections across the apex-base axis of the LV.

To recognize structural remodeling after MI, the sections were stained by both hematoxylin and eosin and picosirius red. The amounts of collagen deposition (scar area) were estimated from six cross sections to cover the whole ventricles in each heart using automated image analysis software (Scion, Frederick, MD). Ten high-power fields per sample were analyzed, and the results were totaled for each animal.

**Immunohistochemistry.** Immunostaining of MK in paraffin sections was performed as described previously (12). Exposure to secondary antibody conjugated with goat anti-rat IgG (Jackson Laboratory, Bar Harbor, ME) was followed by incubation with biotinytyramide and streptavidin-horseradish peroxidase (NEN Life Science Products, Boston, MA) to enhance the immunoreactive signals. The specificity of immunostaining for MK was confirmed by absorption of the anti-MK antibodies with recombinant MK, followed by heparin-sepharose affinity chromatography (12).

Immunohistochemical studies of von Willebrand factor (vWF) and CD31 were used to detect newly developed microvessels. The frozen sections (5- $\mu$ m slices) were incubated overnight with the rat-anti-mouse vWF antibody (Santa Cruz, CA) or with the rat-anti-mouse CD31 antibody (BD Biosciences, Franklin Lakes, NJ) then exposed to the secondary antibody conjugated with goat anti-rat IgG (BD Biosciences). The images were analyzed by two investigators who were blinded with respect to the identification of the groups. The results were expressed as average numbers of capillaries per square millimeter.

**Echocardiography.** Transthoracic echocardiography was performed with a Nemio 20 (Toshiba Medical, Tokyo, Japan) to evaluate global cardiac function before and after MI creation. Mice were lightly anesthetized with diethyl ether and placed in the supine position on a heating pad. The level of anesthesia was kept very light to maintain regular spontaneous respiration and to avoid compromising hemodynamic conditions (13). A 12-MHz transducer was applied to the left hemithorax, and two-dimensional targeted M-mode tracings were recorded. The data were analyzed by an observer blinded to the treatment and genotype of mouse.

**MK protein and antibodies.** Human recombinant MK protein was generated and purified as previously described (12). Monoclonal antibodies against mouse MK were raised by injection of the purified protein into rabbits and were refined by affinity chromatography on protein-A and MK columns. Antibodies were specific to MK and did not react with PTN/HB-GAM.

**Culture of human umbilical vein endothelial cells.** Human umbilical vein endothelial cells (HUVEC) were purchased (Iwaki, Tokyo, Japan) and maintained according to an attached manual. Briefly, recovery cells were cultured at 37° in 5% CO<sub>2</sub>-20% O<sub>2</sub> in 5% fetal bovine serum (FBS) supplemented with growth factors, 50 U/ml penicillin, and 50  $\mu$ g/ml streptomycin. HUVEC at the

third or fourth passage were used for the *in vitro* Matrigel assay and for the Western blotting.

**Western blot analysis.** Western blot analysis was performed to evaluate protein levels. LV tissue homogenates were subjected to SDS-PAGE on a 7.5% polyacrylamide gel, and proteins were electroblotted on polyvinylidene fluoride (PVDF) membranes (Atto, Tokyo, Japan). After blocking, the membrane was incubated with primary antibodies: anti-mouse Akt/PKB antibody (Upstate, Lake Placid, NY) anti-diphosphorylated Akt/PKB antibody (Upstate), PI3K (Upstate), anti-mouse ERK antibody (Sigma) anti-diphosphorylated ERK1/2 antibody (NEN Life Science Products), hypoxia inducible factor (HIF)-1 $\alpha$  (Bethyle, Montgomery, TX), JNK (Cell Signaling Technology, Boston, MA), P38 (Cell Signaling Technology), Bcl-2, Bad, and Bax (Santa Cruz Biotechnology, Santa Cruz, CA) and then exposed to biotinylated anti-mouse IgG (Sigma, St. Louis, MO), horseradish peroxidase-conjugated streptavidin (Amersham Pharmacia Biotech, Little Chalfont, UK), and enhanced chemiluminescence reagent (Amersham Pharmacia Biotech).

To detect Akt and ERK1/2 proteins *in vitro*, cultured HUVEC were lysed in SDS sample buffer, the cell lysate was subjected to SDS-PAGE on a 7.5% polyacrylamide gel, and proteins were electroblotted on PVDF membrane. The membrane was sequentially immunoblotted as described above. The intensity of the bands was quantified by densitometry (Atto).

**Matrigel angiogenesis assays.** For *in vitro* assay, the maintaining medium of confluent HUVEC was changed into 0.5% FBS in endothelial cell basal medium (EBM)-2 without supplemented growth factors. Twenty-four hours later, the medium was then aspirated and the cells were washed twice with phosphate-buffered saline (PBS), trypsinized, and plated in wells coated with growth factor-depleted Matrigel (Becton Dickinson, Bedford, MA) (18) in 0.5% FBS in EBM-2 without growth factors. The HUVEC were then treated with either 100 ng/ml MK, 100 ng/ml basic FGF (bFGF; positive control), or PBS (control). At 6 h later, the plates were photographed, and the extent of tube formation was qualitatively assessed.

To assess the angiogenic efficacy *in vivo*, C57/BL6 mice were anesthetized with pentobarbital (100 mg/kg *ip* injection). The growth factor-depleted Matrigel was mixed with 20 U/ml heparin (Elkins Sinn, Cherry Hill, NJ) and either 500 ng/ml MK, 500 ng/ml bFGF (positive control), or PBS (control). Matrigel mixture (0.5 ml) was injected subcutaneously in the abdominal midline using sterile conditions. Fourteen days later, the pellets were then collected with a piece of underlying abdominal wall, fixed with paraformaldehyde for 2 h, and processed for paraffin embedding. The sections cut into 5  $\mu$ m thickness were stained with hematoxylin and eosin or immunostained with an antibody against vWF. Images of sections at  $\times 40$  magnification were photographed with a digital camera and analyzed using automated image analysis software. Ten random high-power fields were analyzed, and the results were totaled for each animal.

**Real-time PCR.** To quantify mRNA expression of Syndecans (Assay ID: Sdc1 Mm00448918\_m1, Sdc3 Mm01179832\_m1, Sdc4 Mm00488527\_m1), PI3K catalytic subunit p110 (Mm00440894\_m1), Akt, monocyte chemoattractant protein (MCP)-1 (Ccl2 Mm00441242\_m1), matrix metalloproteinases (MMP)-2 (Mm00439508\_m1) and MMP-9 (Mm00600163\_m1) in the LV free wall of mouse hearts and HUVEC, we performed a real-time PCR assay (Perkin-Elmer ABI Prism 7700) (27). 18s mRNA was used as an internal control. Sequence-specific probes were purchased from Applied Biosystems (Foster City, CA).

**Statistic analysis.** All values are expressed as means  $\pm$  SE. Statistical comparisons among the groups were performed by ANOVA with Bonferroni post hoc tests. Comparisons between two groups were made using unpaired Student's *t*-test. The cumulative survival rate of mice after MI creation was analyzed by Kaplan-

Meier method with the long-rank procedure. Probability values of  $<0.05$  were considered significant.

## RESULTS

**MK expression pattern in chronic phase.** We evaluated the time course of MK expression after MI. The protein expression gradually increased, became apparent at 7 days, and persisted until 14 days (Fig. 1A, top). mRNA expression levels of MK were elevated from 3 days (4.0-fold;  $P < 0.05$  vs. sham) to 14 days (7.2-fold;  $P < 0.05$  vs. sham; Fig. 1A, bottom).

**Survival rate after MI is improved by exogenous MK treatment.** In MKKO mice, most animals (7 of 8) died by 7 days after MI, whereas the survival rate of WT mice was 44% at 28 days [WT with no treatment (WT-NT) in Fig. 1B]. Pump failure or ventricular rupture occurred more frequently in MKKO (5 of 7) than in WT (3 of 10) mice.

To examine the therapeutic potential of MK treatment after MI, we subcutaneously administered MK protein using an osmotic pump to MKKO mice. The survival rate of MKKO mice was significantly improved by supplemental treatment of MK protein [knockout (KO)-MK in Fig. 1B]. We further examined the effect of MK treatment on WT mice. At 24 h after MI, there was no significant difference of the serum cTnT level between WT-NT and MK treatment (WT-MK) groups (data not shown). Surprisingly, the survival rate was significantly improved to 90% by MK ( $P < 0.05$ ; WT-MK in Fig. 1B). Consistent with this phenomenon, the serum brain natriuretic peptide (BNP) level at 28 days after MI in WT-MK mice was significantly lower than that of WT-NT ( $129 \pm 5$  pg/dl vs.  $370 \pm 98$  pg/dl;  $P < 0.05$ ; Fig. 1C).

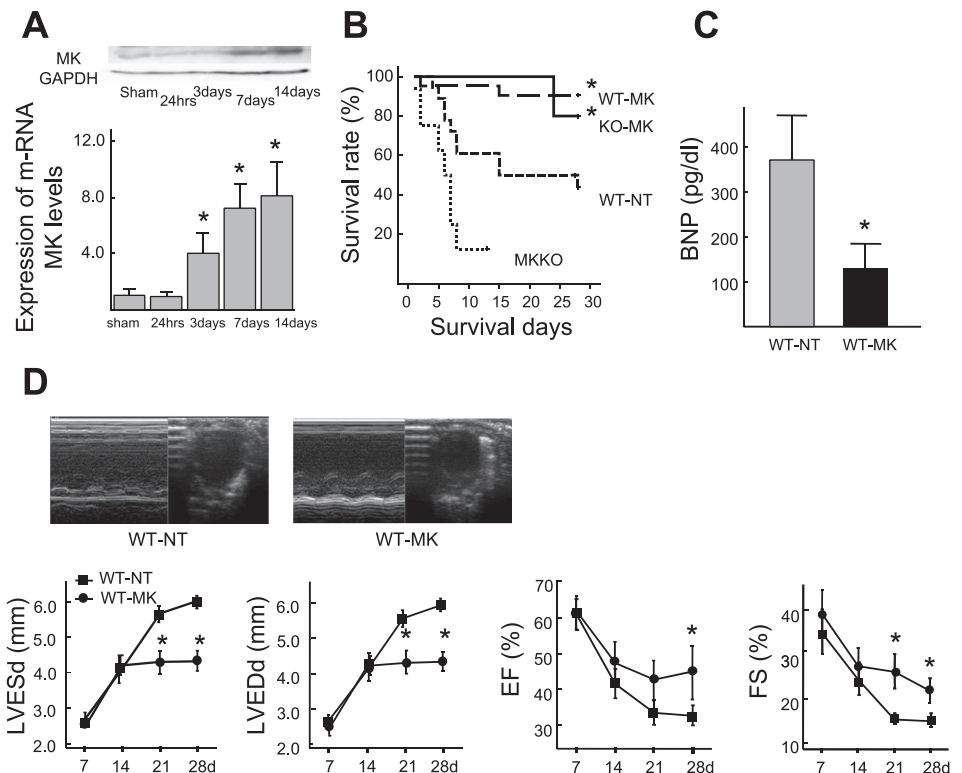
**MK treatment suppressed cardiac dysfunction and prevented progression of heart failure after MI.** Figure 1D summarizes the parameters of echocardiography 7–28 days after MI. Without MK treatment (WT-NT), LV end-diastolic diameter (LVEDd) and LV end-systolic diameter (LVESd) were progressively increased, whereas ejection fraction (EF) and fractional shortening (FS) were progressively decreased during the entire follow-up period. This deterioration was prevented by MK treatment (WT-MK). LVEDd and LVESd at 28 days in WT-MK ( $4.3 \pm 0.5$  mm and  $3.6 \pm 1.0$  mm) were significantly smaller than those in WT-NT ( $6.0 \pm 0.4$  mm and  $5.3 \pm 0.4$  mm;  $P < 0.05$ ). EF and FS at 28 days in WT-MK ( $44.3 \pm 10.1\%$  and  $21.2 \pm 5.4\%$ ) were significantly better than those in WT-NT ( $32.1 \pm 0.6\%$  and  $15.3 \pm 0.3\%$ ;  $P < 0.05$ ).

**Exogenous MK treatment inhibits LV remodeling and enhances neovascularization in WT mice after MI.** To estimate LV remodeling, we first examined fibrosis. The area of collagen deposition quantified by picrosirius red staining at 28 days after MI in WT-MK was significantly smaller than that in WT-NT (Fig. 2A). Incidence of collagen deposition in WT-NT was expanded not only in the infarct zone but also in noninfarcted remote myocardium (Fig. 2A).

We next examined the gene expression of MMPs in the LV tissue. The MMP-9 mRNA level at 28 days after MI was significantly lower in WT-MK than in WT-NT ( $5.4 \pm 1.82$  vs.  $2.2 \pm 0.87$ ;  $P < 0.05$ ; Fig. 2B). The MMP-2 mRNA level at 28 days after MI in WT-MK tended to be lower than that in WT-NT although the difference did not reach a statistical significance (Fig. 2B).

Neovascularization was evaluated by means of immunohistochemistry. The CD31-immunopositive microvessel popula-

Fig. 1. Midkine (MK) expression pattern after myocardial infarction (MI) and consequences of MK treatment in terms of survival rate, serum brain natriuretic peptide (BNP), and echocardiographic assessments. A: protein expression of MK was identified by Western blotting in left ventricular (LV) tissue of wild-type (WT) mice. The photograph shown is a representative of 5 independent experiments. mRNA expression of MK (normalized to 18S) was measured by RT-PCR and summarized in the graph.  $*P < 0.05$  vs. sham. B: survival rate estimated by Kaplan-Meier method in WT with no treatment (WT-NT;  $n = 18$ ), WT treated with MK (WT-MK;  $n = 21$ ), MK knockout mice (MKKO;  $n = 8$ ), and MKKO treated with MK (KO-MK;  $n = 5$ ). Survival rates of WT-MK and KO-MK were significantly higher than that of WT-NT ( $P < 0.05$ ). C: serum BNP at 28 days (d) after MI. The values in WT-MK were significantly less than those of WT-NT ( $n = 15$  each). D: LV end-diastolic diameter (LVEDd), LV end-systolic diameter (LVESd), ejection fraction (EF), and fractional shortening (FS) measured in echocardiography at 7, 14, 21, and 28 days after MI. Values are means  $\pm$  SD of WT-NT ( $n = 8$ ) and WT-MK ( $n = 9$ ). LVEDd and LVESd in WT-MK at 21 and 28 days were significantly smaller than those in WT-NT. EF and FS in WT-MK at 28 days were significantly better than those in WT-NT.  $*P < 0.05$  vs. WT-NT.



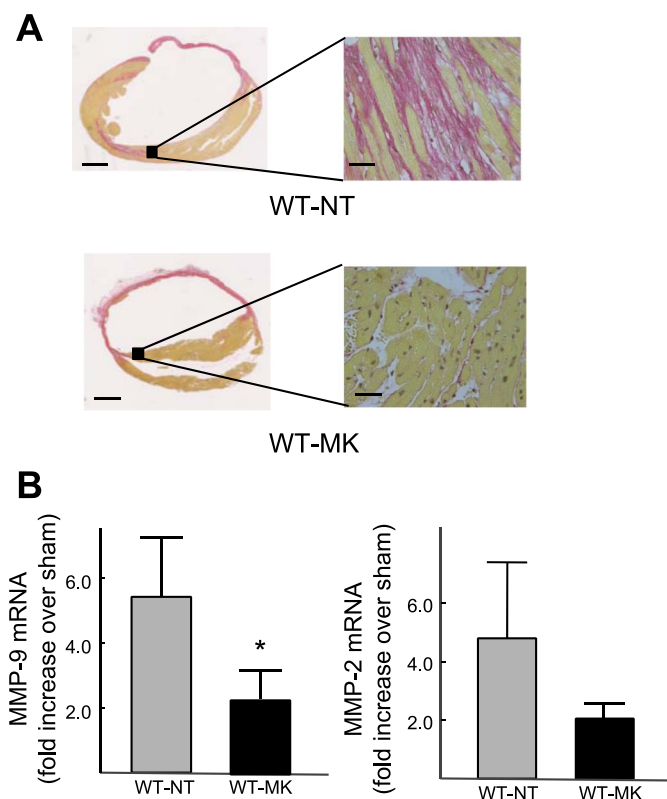


Fig. 2. Fibrosis and mRNA expression of matrix metalloproteinase (MMP)-2 and MMP-9 in ventricles at 28 days after MI. *A*: representative cross section of the ventricles in a WT-NT and WT-MK mouse stained by picrosirius red. The incidence of collagen deposition in the WT-MK was less expanding in the noninfarct area. Left scale bar, 2 mm; right scale bar, 50  $\mu$ m. *B*: mRNA levels (normalized to 18S) of MMP-2 and MMP-9 in LV tissue after MI. MMP-9 mRNA in WT-MK ( $n = 3$ ) was less than that in WT-NT ( $n = 4$ ). Values are means  $\pm$  SD; \* $P < 0.05$  vs. WT-NT.

tion in the LV tissue at 28 days of WT-MK was significantly larger than that of WT-NT ( $79.2 \pm 9.6$  cells/ $\text{mm}^2$  vs.  $51.2 \pm 9.4$  cells/ $\text{mm}^2$ ;  $P < 0.05$ ; Fig. 3, *A* and *B*). To analyze the association between angiogenic phenomenon in WT-MK and proinflammatory action, we assessed transcript levels of MCP-1 in mouse LV tissue 7 days after MI. The expressions of MCP-1 mRNA in WT-MK were significantly higher than in WT-NT ( $1.35 \pm .45$  vs.  $0.6 \pm .17$ ;  $P < 0.05$ ; Fig. 3*C*).

To guarantee the above-mentioned protective effect of exogenous MK administration, administered MK must be properly delivered to the injured site of the heart. Figure 3*D* shows the localization of MK protein administered via an osmotic pump in a KO-MK mouse. The infused MK protein was localized in residual cardiomyocytes in the peri-infarct zone, and the MK accumulation area was roughly consistent with the CD31-enriched area.

*Exogenous MK treatment enhances PI3K/Akt and MAPK signaling.* Enhanced neovascularization by MK treatment prompted us to examine the expression of cell surface molecules (syndecans) and intracellular ones (PI3K, Akt, ERK, p38, and HIF-1 $\alpha$ ) that have relation to angiogenesis. The expressions of syndecans mRNA in LV tissue of WT-MK were significantly higher than in WT-NT 28 days after MI [syndecan-1 (Synd-1),  $8.2 \pm 4.0$ - vs.  $3.2 \pm 1.3$ -fold; syndecan-3 (Synd-3),  $2.3 \pm 0.7$ - vs.  $1.2 \pm 0.2$ -fold;

and syndecan-4 (Synd-4),  $1.4 \pm 0.38$  vs.  $0.83 \pm 0.2$ ;  $P < 0.05$ . Values are normalized to sham] (Fig. 4).

Although there were no substantial differences of expressions of total PI3K and Akt between WT-MK and WT-NT, phosphorylation of PI3K (p-PI3K) and p-Akt was significantly increased in WT-MK (by 76.2% and 61.3%, respectively;  $P < 0.05$ ) compared with WT-NT (Fig. 5*A*). Akt phosphorylation was remarkably reduced in the MKKO compared with WT at 24 h after MI ( $0.23 \pm 0.09$  vs.  $0.9 \pm 0.29$ ;  $P < 0.05$ ; Fig. 5*A*). p-Akt was localized in the microvessel area in WT-MK (Fig. 5*B*). The expression of p-ERK1/2 and p-p38 in WT-MK were significantly higher than in WT-NT (p-ERK1/2,  $1.48 \pm 0.75$  vs.  $0.57 \pm 0.18$ ; p-p38MAP,  $1.98 \pm 0.44$  vs.  $0.21 \pm 0.054$ ;  $P < 0.05$ ; Fig. 5*C*).

Expression of the transcription factor HIF-1 $\alpha$  was also examined. HIF-1 $\alpha$  expression was remarkably increased in WT-MK ( $0.085 \pm 0.041$  vs.  $0.028 \pm 0.013$ ;  $P < 0.05$ ; Fig. 5*D*).

*Exogenous MK treatment reduced apoptosis.* The cellular consequence after MK administration was further evaluated as

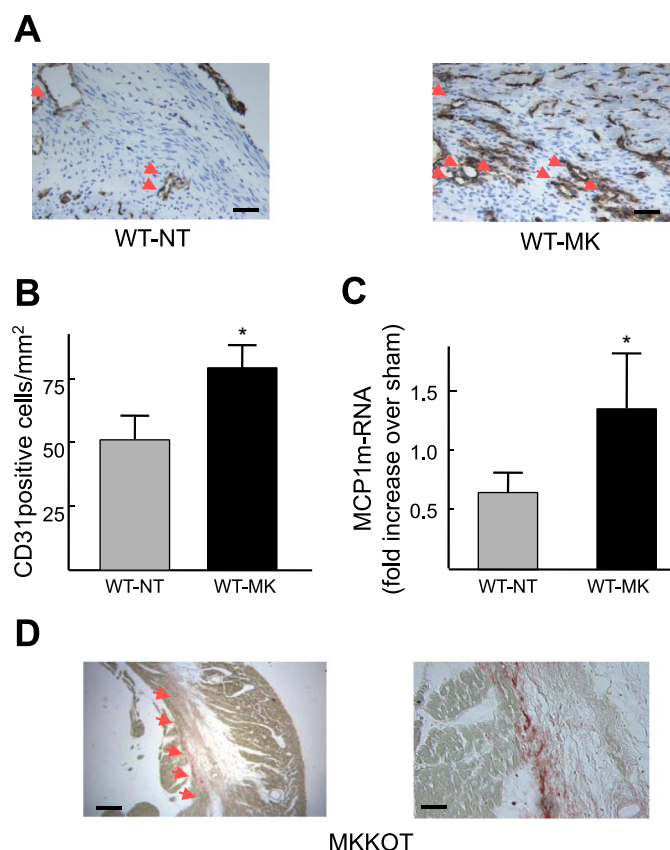


Fig. 3. Neovascularization and localization of infused MK in ischemic heart after MI. *A*: representative immunolabeling pictures for CD31 in LV free wall sections from a WT-NT and a WT-MK mouse 28 days after MI. Arrows indicate CD31-positive microvessels in the peri-infarct zone. Scale bar, 100  $\mu$ m. *B*: density of CD31-positive capillaries in the peri-infarct zone. Values are means  $\pm$  SE of WT-NT ( $n = 5$ ) and WT-MK ( $n = 7$ ). \* $P < 0.05$  vs. WT-NT. The capillary density in WT-NT was significantly less than that of WT-MK. *C*: quantitative analysis of monocyte chemoattractant protein (MCP)-1 gene expression. The expression of mRNA (normalized to 18S) in WT-MK was significantly increased compared with that of WT-NT. *D*: localization of infused MK in the LV peri-infarct zone of a KO-MK mouse. Arrows indicate MK localization in the section of low (*left*) and high (*right*) magnification. Left scale bar, 100  $\mu$ m; right scale bar, 50  $\mu$ m. MKKOT, MKKO mouse treated with exogenous MK.

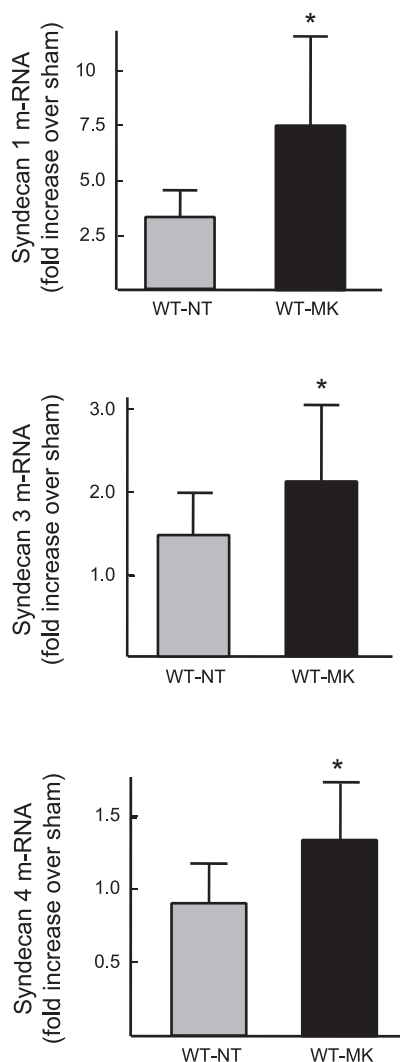


Fig. 4. Expressions of syndecans by MK treatment after MI. Quantitative analysis of syndecan-1, -3, and -4 mRNA expression (normalized to 18S) in the MK treatment hearts was significantly increased compared with that of WT-NT. The data are shown as means  $\pm$  SD; \* $P < 0.05$  vs. WT-NT.

to apoptotic changes in the LV tissue. Terminal deoxynucleotidyl transferase dUTP-mediated nick-end labeling (TUNEL)-positive cells were markedly decreased in WT-NT at 28 h after MI (Fig. 6A). The bax-to-bcl-2 expression ratio of the LV tissue in WT-MK was significantly suppressed compared with that of WT-NT ( $0.72 \pm 0.37$  vs.  $1.46 \pm 0.32$ ;  $P < 0.05$ ; Fig. 6B). p-Bad was significantly increased in WT-MK compared with WT-NT ( $1.0 \pm 0.2$  vs.  $1.2 \pm 0.2$ ;  $P < 0.05$ ; Fig. 6C).

**Angiogenic activity of MK in Matrigel assay in vitro and in vivo.** To confirm the ability of MK to enhance angiogenesis, we first examined the effect of exogenous MK on the formation of vascular structure of HUVEC in an in vitro Matrigel assay. Treatment of HUVEC with 100 ng/ml MK for 6 h resulted in a considerable acceleration of the formation of visible rings and cords of cells on growth factor-depleted Matrigel in the absence of serum. This enhancement of tubular network formation by MK was comparable with the effect of 100 ng/ml bFGF (Fig. 7A). We also examined the effect of MK on the activation of Akt in HUVEC by Western blotting (Fig. 7B). Treatment of HUVEC with 100 ng/ml MK for 6 h caused a

significant increase of p-Akt (by 68.2% from control;  $P < 0.05$ ), and this upregulation was reversed completely by the concomitant application of 30 nmol/l wortmannin, a specific inhibitor of PI3K. The network formation of HUVEC enhanced by MK was reversed by wortmannin (Fig. 7A).

To assess the angiogenic properties of MK in vivo, we measured the extent of vessel invasion into Matrigel pellets implanted in mouse abdominal walls. The incorporation of 500 ng/ml MK into the Matrigel resulted in a significant increase of vessels seen after 14 days compared with that of control pellets. The increase of capillary density by MK, which was measured by immunostaining for vWF in the pellets, was comparable with the effect of 100 ng/ml bFGF (Fig. 7, C and D).

## DISCUSSION

The present study demonstrated that MK plays a crucial role in the cardiac remodeling after MI. Exogenous in vivo application of MK to WT mice after MI activated PI3K/Akt and MAPKs. Concomitantly, exogenous MK enhanced neovascularization in the peri-infarct zone, ameliorated LV fibrosis and dysfunction, and improved survival rate. Moreover, MKKO mice showed a higher mortality and less activation of Akt compared with WT mice. The angiogenic action of MK, which was associated with Akt activation, was confirmed in in vitro experiments using HUVEC. Taken together, these results suggest that MK exerts a protective effect against the ventricular remodeling after MI through the activation of angiogenesis.

Angiogenesis is the most important repair process of tissues subjected to ischemic insult, and stimulation of neovascularization is expected to reduce ventricular remodeling and dysfunction after MI (17, 36). The intracellular signaling molecules responsible for the neovascularization include PI3K/Akt and MAPKs (13, 24, 28). Among them, Akt is a serine/threonine protein kinase that is activated by a number of growth factors (e.g., VEGF, hepatocyte growth factor, and bFGF) in a PI3K-dependent manner. Akt regulates multiple critical steps in angiogenesis, including endothelial cell survival, migration, and capillary-like structure formation (32). HIF-1 $\alpha$  exists downstream of Akt and regulates expression of many angiogenesis-related genes including those of VEGF and FLT (2, 9, 18, 20). It is of note that HIF-1 $\alpha$  upregulates MK expression (30). Therefore, the potent angiogenic activity of MK as shown in the present experiments using mouse MI models would be explained primarily by the PI3K-Akt signaling axis like other growth factors. The marked reduction of Akt phosphorylation in MKKO mice suggested that MK has critical role to activate Akt, and indeed, exogenous treatment of MK for WT mice caused remarkable acceleration of Akt and PI3K activation after MI. In addition to these in vivo data, the in vitro action of exogenous MK on HUVEC to activate Akt and promote tubulogenesis was prevented by wortmannin, a specific inhibitor of PI3K.

Angiogenesis is deeply associated with inflammatory reaction (1). For instance, monocyte/macrophages accumulation is a critical player in both capillary sprouting and collateral artery growth. These inflammatory cells produce a variety of angiogenic cytokines and growth factors upon

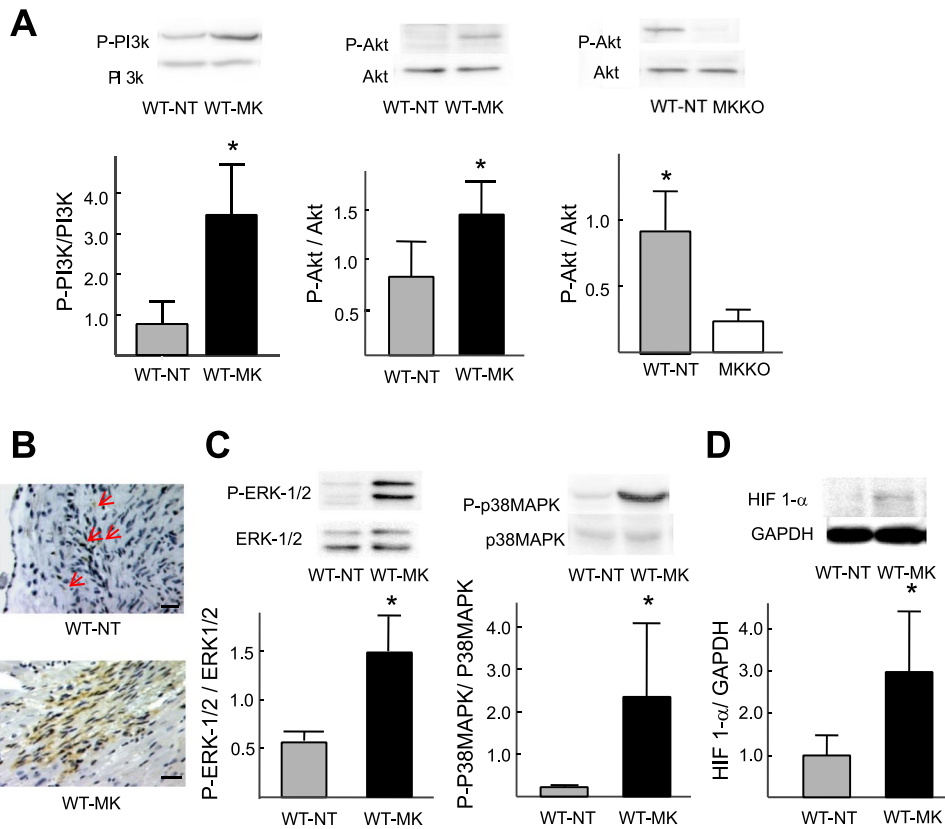


Fig. 5. Consequences of MK treatment in terms of phosphatidylinositol 3-kinase (PI3K)/Akt pathway, MAPK family, and hypoxia inducible factor (HIF)-1 $\alpha$  expressions. **A**: Western blots of PI3K and Akt in LV at 28 days after MI. The amounts of phosphorylated (p) PI3K and p-Akt in WT-MK were significantly larger than those in WT-NT ( $n = 4$  each). The expression of p-Akt in MKKO was significantly less than in WT-NT. Graphs are summaries of densitometric values. **B**: immunohistochemistry of p-Akt in WT-NT and WT-MK. Scale bar, 100  $\mu$ m. **C**: representative Western blots showing ERK1/2 phosphorylation and p38 MAPK phosphorylation. Values are means  $\pm$  SE ( $n = 4$ ). **D**: expression of HIF-1 $\alpha$  was significantly increased in WT-MK compared with WT-NT. \* $P < 0.05$  vs. WT-NT. Arrows indicate microvessel area.

activation. MCP-1, TNF- $\alpha$ , bFGF, and MMPs belong to their repertoire (14, 37). In this study, the expression pattern of MK matched with the macrophage infiltration in acute or subacute inflammation phase after MI (14), and the survival rate of MKKO mice was significantly worse than WT in this phase (Fig. 1). From these data, there is a possibility that MK is also produced by inflammatory cells. In fact, Narita et al. (26) showed that MK is expressed by macrophages in neointima of hypercholesterolemic rabbits. On the other hand, MK is known to promote the chemotaxis of neutrophils or the migration of macrophages (12). Our laboratory has shown previously that MK has a critical role in neointima formation by enhancing the recruitment of inflammatory cells (12). MK also induces activation of MCP-1 and mediates the inflammatory reaction in the kidney subjected to ischemia-reperfusion (31). These observations suggest that the potent angiogenic activity of MK in the heart after MI is mediated in part by its proinflammatory action.

Is associated with an inflammatory reaction, which is a prerequisite for healing and scar formation. There is complex interplay among many factors involved in the reaction. In terms of LV remodeling and dysfunction after MI, inflammation can induce either undesirable or beneficial effects (10, 14). The former effect is the result of the progression of myocardial injury, whereas the latter one is the result mainly of an enhancement of angiogenesis, and the final consequence is determined by their balance under a variety of pathological conditions (7). Among MK-associated inflammatory molecules, MCP-1 has long been considered to play a deleterious role in postinfarct LV dysfunction and remodeling. Morimoto et al. (21), however, have shown in

their study using transgenic mice that the cardioselective overexpression of MCP-1 prevents LV dysfunction and remodeling after MI through an enhancement of neovascularization.

We also found in the present study that the expression of syndecans was enhanced in MK-treated WT mice. Syndecans are membrane-bound heparan sulfated proteoglycans, and implicated in angiogenesis. For example, mice lacking Synd-4 show impaired angiogenesis, and Synd-2 is required for angiogenic spouting during zebrafish development (3, 6). It is interesting that MK binds to syndecans (6). Furthermore, a recent study by Vanhoutte et al. (35) using mice of targeted Synd1 deletion and adenovirus Synd1 gene overexpression has demonstrated that increased the expression of Synd-1 in MI prevents inverse healing, thereby reducing cardiac dilatation and dysfunction after MI. Accordingly, MK-induced syndecan family could contribute the amelioration of LV remodeling and dysfunction after MI through a similar mechanism. Beside syndecans, MK binds to other cell surface molecules. The MK receptor is thought to be a molecular complex including syndecan family members; protein-tyrosine phosphatase- $\zeta$ , a chondroitin sulfate proteoglycan; members of the low density lipoprotein receptor-related protein family; and anaplastic lymphoma kinase, a receptor-type tyrosine kinase (15, 19, 22, 24). Biological significance of these molecules after MI remains to be verified.

Fukui et al. (8) recently showed that MK has therapeutic effects for cardiac remodeling after MI. Although they did not show the detailed molecular mechanisms, the results were similar with our data in the point that the angiogenic

effect of MK showed preventive action for LV remodeling. In addition to their data, we have shown the involvement of the PI3K/Akt pathway in MK-mediated angiogenesis. Furthermore, the antiapoptotic effects of MK in MI model were demonstrated in the present study. We previously showed in mouse acute MI model induced by ischemia-reperfusion that MK ameliorates acute myocardial injury through its potent antiapoptotic action (13). In this study, we also found that MK treatment reduced apoptotic reaction in the chronic phase of ligation model. The signaling pathways of angiogenesis and apoptosis overlap and cross-talk each other: MAPKs especially initiate the activation of Bax and Bcl-2 (29). Bad, a proapoptotic member of the Bcl-2 family, is displaced by Bax from binding to Bcl-2 and Bcl-XL (38). In addition to MAPKs, the phosphorylated Akt inhibits the apoptotic effects of Bad (5). These facts suggest that the MK could prevent remaining myocardiocytes from apoptosis via

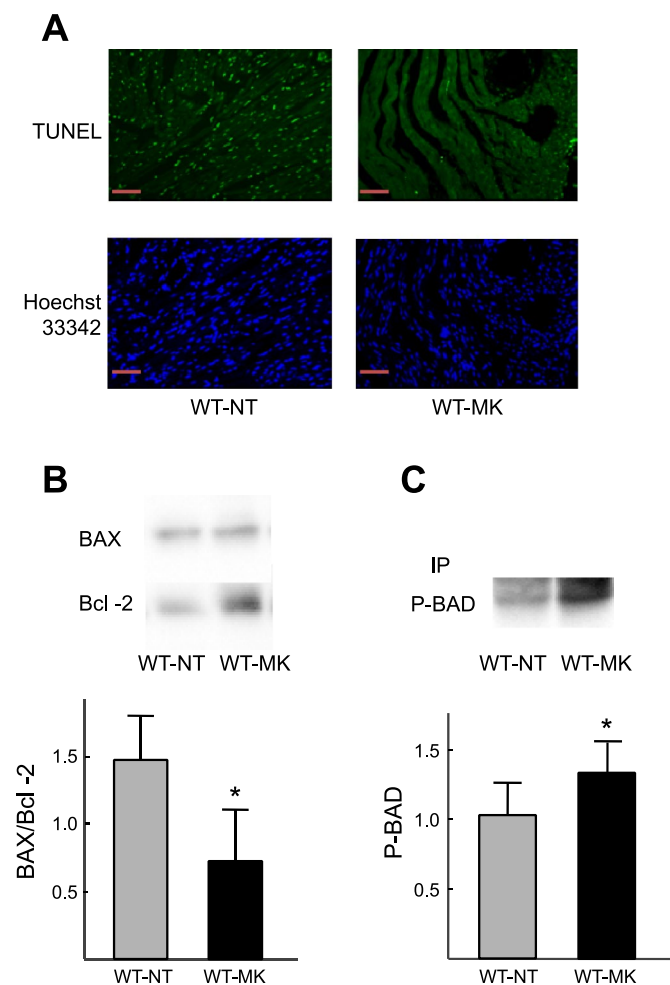


Fig. 6. Effects of apoptotic change in the postinfarct heart. **A**: terminal deoxynucleotidyl transferase dUTP-mediated nick-end labeling (TUNEL) staining in the peri-infarct area of WT-NT and WT-MK. WT-MK shows a marked decrease of TUNEL-positive apoptotic cells. **B**: representative Western blots of Bcl-2 and Bcl-2-associated X protein (Bax). The ratio of Bcl-2 to Bax in the WT-MK ( $n = 4$ ) was significantly decreased compared with that in WT-NT ( $n = 4$ ). **C**: representative Western blots of p-bcl-xl/bcl-2-associated death promoter (Bad). The p-Bad in the WT-MK ( $n = 4$ ) was significantly increased compared with that in WT-NT ( $n = 4$ ). Values are means  $\pm$  SD.  $*P < 0.05$  vs. WT-NT. Scale bars, 100  $\mu$ m. IP, immunoprecipitation.

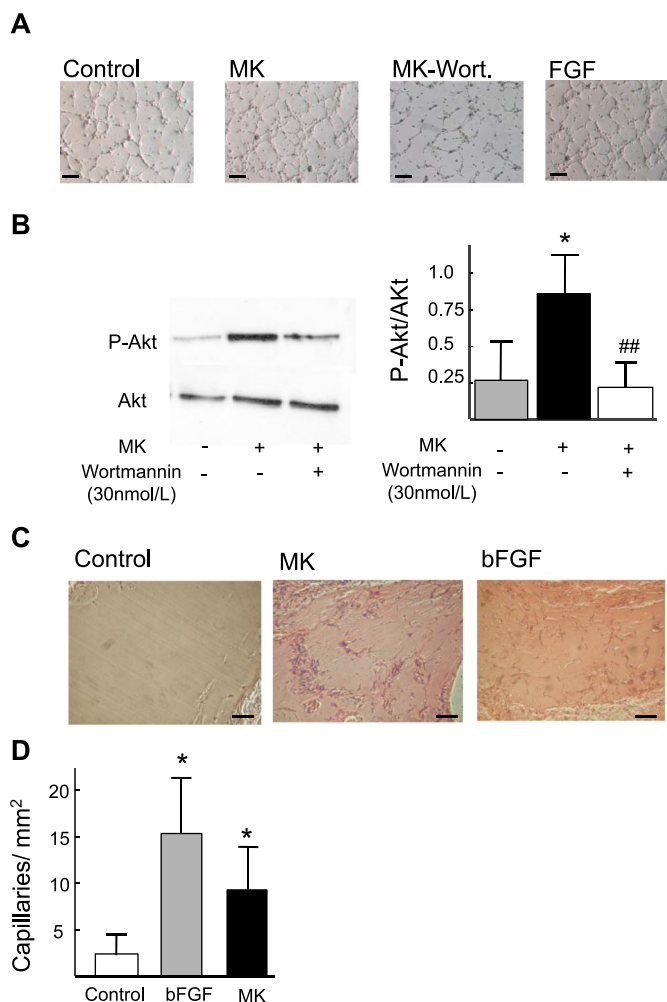


Fig. 7. Matrigel assays in vitro and in vivo. **A**: in vitro assay to see the formation of vascular structure of human umbilical vein endothelial cells (HUVEC). HUVEC were seeded on growth factor-depleted Matrigel in the absence of serum and in the presence of either 100 ng/ml MK ( $n = 8$ ), 100 ng/ml basic (b)FGF (positive control;  $n = 8$ ), or vehicle (control;  $n = 6$ ) and were photographed after 6 h. MK-treated and bFGF-treated cells showed much more extensive ring and cord formation than control cells. Scale bars, 50  $\mu$ m. **B**: activation of Akt in HUVEC assessed by Western blots in Matrigel assay in vitro. Application of 100 ng/ml MK for 6 h caused a significant upregulation of p-Akt, and this upregulation was reversed by concomitant application of 30 nmol/l wortmannin (Wort; means  $\pm$  SE,  $n = 5$  each).  $*P < 0.01$  vs. control.  $##P < 0.01$  vs. MK alone. **C**: in vivo assay is sections from control and MK- and bFGF-impregnated Matrigel pellets (hematoxylin and eosin). Treatment with either MK (500 ng/ml) or bFGF (100 ng/ml) resulted in a considerable increase in vessel invasion. Scale bar, 100  $\mu$ m. **D**: density of newly formed vessels in Matrigel assessed by von Willebrand factor immunostaining (means  $\pm$  SE;  $n = 10$  each).  $*P < 0.05$  vs. control.

MAPKs and Akt pathways. The potent angiogenic and antiapoptotic activities of MK in the chronic phase of MI may synergistically exert effects on the prevention of LV remodeling and dysfunction in favor of long-term survival. The beneficial effects of exogenous MK application would provide a new perspective for the innovation in the treatment of MI.

#### ACKNOWLEDGMENTS

We thank Drs. H. Ohshima and M. Jijiwa for critical advice and S. Ikematsu for providing MK antibody. We thank T. Koike and A. Takahashi for technical assistance.

## GRANTS

This work was supported by grants from the Ministry of Education, Culture, Sports, Science and Technology Japan (to M. Horiba).

## REFERENCES

1. Arras M, Ito WD, Scholz D, Winkler B, Schaper J, Schaper W. Monocyte activation in angiogenesis and collateral growth in the rabbit hindlimb. *J Clin Invest* 101: 40–50, 1998.
2. Carmeliet P, Dor Y, Herbert JM, Fukumura D, Brusselmans K, Dewerchin M, Neeman M, Bono F, Abramovitch R, Maxwell P, Koch CJ, Ratcliffe P, Moons L, Jain RK, Collen D, Keshert E. Role of HIF-1 alpha in hypoxia-mediated apoptosis, cell proliferation and tumour angiogenesis. *Nature* 395: 525, 1998.
3. Chen E, Hermanson S, Ekker SC. Syndecan-2 is essential for angiogenic sprouting during zebrafish development. *Blood* 103: 1710–1719, 2004.
4. Choudhuri R, Zhang HT, Donnini S, Ziche M, Bicknell R. An angiogenic role for the neurokines midkine and pleiotrophin in tumorigenesis. *Cancer Res* 57: 1814–1819, 1997.
5. Datta SR, Dudek H, Tao X, Masters S, Fu HA, Gotoh Y, Greenberg ME. Akt phosphorylation of BAD couples survival signals to the cell-intrinsic death machinery. *Cell* 91: 231–241, 1997.
6. Echtermeyer F, Streit M, Wilcox-Adelman S, Saoncella S, Denhez F, Detmar M, Goetinck PF. Delayed wound repair and impaired angiogenesis in mice lacking syndecan-4. *J Clin Invest* 107: R9–R14, 2001.
7. Frangogiannis NG, Smith CW, Entman ML. The inflammatory response in myocardial infarction. *Cardiovasc Res* 53: 31–47, 2002.
8. Fukui S, Kitagawa-Sakakida S, Kawamata S, Matsumiya G, Kawaguchi N, Matsuura N, Sawa Y. Therapeutic effect of midkine on cardiac remodeling in infarcted rat hearts. *Ann Thorac Surg* 85: 562–570, 2008.
9. Gerber HP, Condorelli F, Park J, Ferrara N. Differential transcriptional regulation of the two vascular endothelial growth factor receptor genes, Flt-1, but not Flk-1/KDR, is up-regulated by hypoxia. *J Biol Chem* 272: 23659–23667, 1997.
10. Giugliano GR, Giugliano RP, Gibson CM, Kuntz RE. Meta-analysis of corticosteroid treatment in acute myocardial infarction. *Am J Cardiol* 91: 1055–1059, 2003.
11. Henry TD, Annex BH, McKendall GR, Azrin MA, Lopez JJ, Giordano FJ, Shah PK, Willerson JT, Benza RL, Berman DS, Gibson CM, Bajamonde A, Rundle AC, Fine J, McCluskey ER. The VIVA trial: Vascular endothelial growth factor in Ischemia for Vascular Angiogenesis. *Circulation* 107: 1359–1365, 2003.
12. Horiba M, Kadomatsu K, Nakamura E, Muramatsu H, Ikematsu S, Sakuma S, Hayashi K, Yuzawa Y, Matsuo S, Kuzuya M, Kaname T, Hirai M, Saito H, Muramatsu T. Neointima formation in a restenosis model is suppressed in midkine-deficient mice. *J Clin Invest* 105: 489–495, 2000.
13. Horiba M, Kadomatsu K, Yasui K, Lee JK, Takenaka H, Sumida A, Kamiya K, Chen S, Sakuma S, Muramatsu T, Kodama I. Midkine plays a protective role against cardiac ischemia/reperfusion injury through a reduction of apoptotic reaction. *Circulation* 114: 1713–1720, 2006.
14. Jugdutt BI. Ventricular remodeling after infarction and the extracellular collagen matrix: when is enough enough? *Circulation* 108: 1395–1403, 2003.
15. Kadomatsu K, Muramatsu T. Midkine and pleiotrophin in neural development and cancer. *Cancer Lett* 204: 127–143, 2004.
16. Kadomatsu K, Tomomura M, Muramatsu T. cDNA cloning and sequencing of a new gene intensely expressed in early differentiation stages of embryonal carcinoma cells and in mid-gestation period of mouse embryogenesis. *Biochem Biophys Res Commun* 151: 1312–1318, 1988.
17. Krzeminski TF, Nozynski JK, Grzyb J, Porc M, Zeglen S, Filas V, Skopinska-Rozewska E, Sommer E, Filewska M. Angiogenesis and cardioprotection after TNFalpha-inducer-Tolpa Peat Preparation treatment in rat's hearts after experimental myocardial infarction in vivo. *Vascul Pharmacol* 43: 164–170, 2005.
18. Li J, Post M, Volk R, Gao Y, Li M, Metais C, Sato K, Tsai J, Aird W, Rosenberg RD, Hampton TG, Sellke F, Carmeliet P, Simons M. PR39, a peptide regulator of angiogenesis. *Nat Med* 6: 49–55, 2000.
19. Maeda N, Ichihara-Tanaka K, Kimura T, Kadomatsu K, Muramatsu T, Noda M. A receptor-like protein-tyrosine phosphatase PTPzeta/RPTPbeta binds a heparin-binding growth factor midkine. Involvement of arginine 78 of midkine in the high affinity binding to PTPzeta. *J Biol Chem* 274: 12474–12479, 1999.
20. Martin C, Yu AY, Jiang BH, Davis L, Kimberly D, Hohimer AR, Semenza GL. Cardiac hypertrophy in chronically anemic fetal sheep: increased vascularization is associated with increased myocardial expression of vascular endothelial growth factor and hypoxia-inducible factor 1. *Am J Obstet Gynecol* 178: 527–534, 1998.
21. Morimoto H, Takahashi M, Izawa A, Ise H, Hongo M, Kolattukudy PE, Ikeda U. Cardiac overexpression of monocyte chemoattractant protein-1 in transgenic mice prevents cardiac dysfunction and remodeling after myocardial infarction. *Circ Res* 99: 891–899, 2006.
22. Muramatsu H, Zou K, Sakaguchi N, Ikematsu S, Sakuma S, Muramatsu T. LDL receptor-related protein as a component of the midkine receptor. *Biochem Biophys Res Commun* 270: 936–941, 2000.
23. Muramatsu T. Midkine (MK), the product of a retinoic acid responsive gene, and pleiotrophin constitute a new protein family regulating growth and differentiation. *Int J Dev Biol* 37: 183–188, 1993.
24. Muramatsu T. Midkine and pleiotrophin: two related proteins involved in development, survival, inflammation and tumorigenesis. *J Biochem (Tokyo)* 132: 359–371, 2002.
25. Nakamura E, Kadomatsu K, Yuasa S, Muramatsu H, Mamiya T, Nabeshima T, Fan QW, Ishiguro K, Igakura T, Matsubara S, Kaname T, Horiba M, Saito H, Muramatsu T. Disruption of the midkine gene (Mdk) resulted in altered expression of a calcium binding protein in the hippocampus of infant mice and their abnormal behaviour. *Genes Cells* 3: 811–822, 1998.
26. Narita H, Chen S, Komori K, Kadomatsu K. Midkine is expressed by infiltrating macrophages in in-stent restenosis in hypercholesterolemic rabbits. *J Vasc Surg* 47: 1322–1329, 2008.
27. Niwa N, Yasui K, Ophhof T, Takemura H, Shimizu A, Horiba M, Lee JK, Honjo H, Kamiya K, Kodama I. Cav3.2 subunit underlies the functional T-type Ca<sup>2+</sup> channel in murine hearts during the embryonic period. *Am J Physiol Heart Circ Physiol* 286: H2257–H2263, 2004.
28. Qi M, Ikematsu S, Maeda N, Ichihara-Tanaka K, Sakuma S, Noda M, Muramatsu T, Kadomatsu K. Haptotactic migration induced by midkine. Involvement of protein-tyrosine phosphatase zeta mitogen-activated protein kinase, and phosphatidylinositol 3-kinase. *J Biol Chem* 276: 15868–15875, 2001.
29. Reddy KB, Nabha SM, Atanaskova N. Role of MAP kinase in tumor progression and invasion. *Cancer Metastasis Rev* 22: 395–403, 2003.
30. Reynolds PR, Mucenski ML, Le Cras TD, Nichols WC, Whitsett JA. Midkine is regulated by hypoxia and causes pulmonary vascular remodeling. *J Biol Chem* 279: 37124–37132, 2004.
31. Sato W, Yuzawa Y, Kadomatsu K, Tayasu T, Muramatsu H, Muramatsu T, Matsuo S. Midkine expression in the course of nephrogenesis and its role in ischaemic reperfusion injury. *Nephrol Dial Transplant* 17 Suppl 9: 52–54, 2002.
32. Shiojima I, Walsh K. Role of Akt signaling in vascular homeostasis and angiogenesis. *Circ Res* 90: 1243–1250, 2002.
33. Solomon AJ, Gersh BJ. Management of chronic stable angina: medical therapy, percutaneous transluminal coronary angioplasty, and coronary artery bypass graft surgery. Lessons from the randomized trials. *Ann Intern Med* 128: 216–223, 1998.
34. Unger EF, Goncalves L, Epstein SE, Chew EY, Trapnell CB, Cannon RO III, Quyyumi AA. Effects of a single intracoronary injection of basic fibroblast growth factor in stable angina pectoris. *Am J Cardiol* 85: 1414–1419, 2000.
35. Vanhoutte D, Schellings MW, Gotte M, Swinnen M, Herias V, Wild MK, Vestweber D, Chorianopoulos E, Cortes V, Rigotti A, Stepp MA, Van de WF, Carmeliet P, Pinto YM, Heymans S. Increased expression of syndecan-1 protects against cardiac dilatation and dysfunction after myocardial infarction. *Circulation* 115: 475–482, 2007.
36. Wang Y, Ahmad N, Wani MA, Ashraf M. Hepatocyte growth factor prevents ventricular remodeling and dysfunction in mice via Akt pathway and angiogenesis. *J Mol Cell Cardiol* 37: 1041–1052, 2004.
37. Yoshida S, Yoshida A, Ishibashi T. Induction of IL-8, MCP-1, and bFGF by TNF-alpha in retinal glial cells: implications for retinal neovascularization during post-ischemic inflammation. *Graefes Arch Clin Exp Ophthalmol* 242: 409–413, 2004.
38. Zha JP, Harada H, Yang E, Jockel J, Korsmeyer SJ. Serine phosphorylation of death agonist BAD in response to survival factor results in binding to 14–3-3 not BGL-X(L). *Cell* 87: 619–628, 1996.
39. Zhao XY, Hu SJ, Li J, Mou Y, Chan CF, Jin J, Sun J, Zhu ZH. rAAV-mediated angiogenin gene transfer induces angiogenesis and modifies left ventricular remodeling in rats with myocardial infarction. *J Mol Med* 84: 1033–1046, 2006.